



Dynamic response and wind loads of a tall building based on wind tunnel tests

Lorenzo Rosa, Gisella Tomasini, Alberto Zasso

Politecnico di Milano, Dipartimento di Meccanica – gisella.tomasini@polimi.it – via La Masa 1, 20156, Milano, Italy.

Politecnico di Milano, Dipartimento di Meccanica – lorenzo.rosa@polimi.it – via La Masa 1, 20156, Milano, Italy.

Politecnico di Milano, Dipartimento di Meccanica – alberto.zasso@polimi.it – via La Masa 1, 20156, Milano, Italy.

Keywords: wind tunnel testing, tall building, wind load, comfort level, modal numerical simulation

ABSTRACT

This paper presents a method, based on the multi-modal approach, to evaluate the dynamic response of a structure and to calculate the wind loads. The method is shown applied on a tall building designed for office use. The set-up methodology allows to calculate the maximum displacements and accelerations of the tower caused by the turbulent wind useful to check the comfort level and to calculate the overall wind loads on the building. The input data of this analysis are the pressure distributions on the external surface of the building and the building modal parameters. An experimental research has been carried out in a boundary layer wind tunnel on a 1:100 scaled model of the building, while the modal parameters have been calculated from a finite element model of the tower. As final output of the methodology, the internal loads acting on the building are evaluated starting from the external loads associated to the pressure distributions and from the inertial loads calculated through the accelerations.

INTRODUCTION

The dynamic response of the structures can be evaluated fully analytically using codes and formulas,

Contact person: Lorenzo Rosa, Politecnico di Milano, via La Masa 1, 20156 Milano, Italy.

tel: +390223998076; fax: +390223998081; E-mail: lorenzo.rosa@polimi.it

for instance ASCE (2008) or Eurocode1 (2004). However, these codes provide good guidance for calculating the along-wind response but little guidance for the critical across-wind and torsional responses. This could be partially attributed to the fact that the across-wind and torsional responses, unlike the along-wind, are given mainly by the aerodynamic pressure fluctuations in the separated shear layers and the wake flow fields, which have prevented, to date, any acceptable direct analytical relation to the oncoming velocity fluctuations (NatHaz, (2008)). Moreover, these methods have limitations because they are often restricted to the first two flexural modes and because they can't account for the effects due to the other tall buildings in the vicinity that could modify the flow acting on the tower itself. For these reasons, a wind tunnel study, associated with a multi-modal numerical simulation, is a valid alternative to calculate the response of a structure, considering also the effects of the torsional modes.

Main aim of the paper is to present a methodology for the evaluation of the dynamic response of a structure and for the calculation of the wind loads. The method in this study is applied to a tall building for office use. The input data of this analysis are the pressure distributions on the external surface of the building and the building modal parameters. The dynamic analysis is carried out through a modal approach which allows to evaluate, known the modal information (frequencies, modal masses, geometry of the FEM model and modal shapes), the response of the tower caused by the turbulent wind, in terms of peak displacements and accelerations of some interesting points of the building. Moreover, starting from the measured external loads associated to the pressure and from the inertial loads calculated through the accelerations, the internal loads acting on the building are evaluated. This analysis allows to identify the most critical load cases actually experienced by the tower which can be used for the structural design.



Figure 1. Test arrangement. The model of the tower and the surrounding in the wind tunnel test section (sx). Close up view of the tower and the force balance (dx).

WIND TUNNEL TESTS

The tower is 138m high and it is manufactured in 1/100 geometric scale (see Figure 1). The value is a compromise between the need to realize models as large as possible and to keep low blockage values (the boundary layer test section is 14x4m). The large dimensions of the model are helpful both in reproducing the geometric details and to achieve a Reynolds Number as near as possible to that of the full-scale condition.

Wind tunnel tests were carried out in a scaled simulation of the natural wind characteristic of the site. At this purpose also the existing buildings within a radius of 500m in the surroundings were added in the set-up. The whole area of the tower and the surrounding was placed on the turntable (diameter 13m). In this way it is possible to investigate all the wind exposures angles (from 0deg to

360 deg with a step of 10deg, Figure 2) without any changing in the test set-up.

In order to simulate the correct turbulence and wind speed vertical profile, passive turbulence generators (spires and roughness elements), were also placed in the wind tunnel, Figure 1.

The tower is manufactured as a “rigid aerodynamic model”, that is a static model that reproduces only the geometry of the full-scale structure (aerodynamic surfaces and details) and not its dynamic behaviour. It is manufactured in alucobond to have high stiffness and high structural frequencies. The experimental set-up allows the measurement of both the surface pressures on the external surface and the global wind loads in terms of forces and moments at its base. The pressures on the external surface are defined by simultaneously measurements in 208 discrete points (pressure taps). Pressure measurements are performed using the high-speed scanning pressure equipment PSI-system 8400 and the ESP miniature pressure scanners. The small dimensions of the scanners allow to place them into the model close to the measuring points, reducing the length of the tubes.

Global forces measurement is carried out by means of a six-component dynamometric force-balance linked at the base of the model (Figure 1). The only joint between the model and the ground is the balance, so all the external forces acting on the tower are measured by the balance, placed on an equipment fixed under the turntable. Pressure and forces are acquired for 100s time history length at the sample rate of 100 Hz.

Global forces on the structure are calculated as non-dimensional aerodynamic coefficients, defined as:

$$C_{FX} = \frac{\bar{F}_X}{\bar{q}_H BH}; C_{FY} = \frac{\bar{F}_Y}{\bar{q}_H BH}; C_{MX} = \frac{\bar{M}_X}{\bar{q}_H BH^2}; C_{MY} = \frac{\bar{M}_Y}{\bar{q}_H BH^2}; C_{MZ} = \frac{\bar{M}_Z}{\bar{q}_H B^2 H}; \quad (1)$$

The dimensions used to calculate the coefficients are the height of the building H and the width at the base B . The reference system and the reduction point for the forces and moments is shown in Figure 2.

DYNAMIC ANALYSIS METHODOLOGY

The dynamic analysis of the tower is carried out through modal approach starting from the pressures measured experimentally in the wind tunnel. The modal approach allows to evaluate, known the modal information (frequencies, modal masses and modal shapes in correspondence of the pressure taps), the response of the tower caused by the turbulent wind, in terms of peak displacements and accelerations in the nodes of the model and in some interesting points of the building (in this case the modal information have been extrapolated from the FEM model). The analysis is carried out, in the time domain, by step by step numerical integration of the motion equations of the tower.

The calculation of the equivalent time in the real structure has been done making equal the reduced frequency from the model to the real:

$$\left[\frac{f \cdot L}{V} \right]_M = \left[\frac{f \cdot L}{V} \right]_R \quad (2)$$

where f is a frequency of the structure and L a geometry dimension. The length of the time history (more than 4500s in real scale) is verified being statistically revealing for the structure, in agreement with the scale factors and the design wind speeds. The first three mode shape of the tower have been considered in this analysis: first mode y -flexural at 0.28Hz, second mode x -flexural at 0.33Hz, third mode torsional at 0.63Hz.

The equations of motion governing the behavior of the structure under wind loads are:

$$\mathbf{M}\ddot{\mathbf{X}}(t) + \mathbf{C}\dot{\mathbf{X}}(t) + \mathbf{K}\mathbf{X}(t) = \mathbf{F}(t) \quad (3)$$

where $\mathbf{X}(t) = [x(t) \ y(t) \ z(t)]^T$ is a $3n \times 1$ vector of time histories: n is the number of nodes (matching with the pressure taps), and $x(t)$, $y(t)$, $z(t)$ are vectors of nodal displacements in x , y , and z

directions respectively. M , C and K are respectively the mass, damping and stiffness matrixes of the structure. $F(t)$ is the vector of the time histories of the pressure forces $F_k(t)$ acting at each k^{th} node (the nodes match with the pressure taps) on the three directions x , y and z . These forces and the moments are obtained calculating the tributary area A_k of each k^{th} pressure tap, calculating the relating projections $\chi_k^x, \chi_k^y, \chi_k^z$ in the three directions x , y , z , and finally integrating the wind pressure (obtained from the wind tunnel tests) over each k^{th} corresponding tributary area A_k to give the three components of force and the three components of moment in each k^{th} node (see the diagram in Figure 2b). The reduction point for the moments is the base point of the reference system (Figure 2a). The pressure forces and moments in their three cartesian components are finally calculated using eq.(4), where h_k is the distance of the k^{th} -node from the base point:

$$\begin{aligned} F_k^{x,y,z}(t) &= p_k(t) \cdot \chi^{x,y,z} \\ M_k^{x,y,z}(t) &= p_k(t) \cdot \chi^{x,y,z} \cdot h_k \end{aligned} \quad (4)$$

According to the modal approach, the vector \mathbf{X} is expressed as:

$$\mathbf{X}(t) = \mathbf{\Phi} \underline{q}(t) \quad (5)$$

where $\mathbf{\Phi}$ ($3n \times 3$) is the matrix of eigenvectors and $\underline{q}(t)$ (3×1) is the vector of generalized displacements:

$$\mathbf{\Phi} = \begin{bmatrix} \phi_1(x_1) & \phi_2(x_1) & \phi_3(x_1) \\ \phi_1(x_2) & \phi_2(x_2) & \phi_3(x_2) \\ \vdots & \vdots & \vdots \\ \phi_1(x_n) & \phi_2(x_n) & \phi_3(x_n) \\ \phi_1(y_1) & \phi_2(y_1) & \phi_3(y_1) \\ \phi_1(y_2) & \phi_2(y_2) & \phi_3(y_2) \\ \vdots & \vdots & \vdots \\ \phi_1(y_n) & \phi_2(y_n) & \phi_3(y_n) \\ \phi_1(z_1) & \phi_2(z_1) & \phi_3(z_1) \\ \phi_1(z_2) & \phi_2(z_2) & \phi_3(z_2) \\ \vdots & \vdots & \vdots \\ \phi_1(z_n) & \phi_2(z_n) & \phi_3(z_n) \end{bmatrix}, \quad \underline{q}(t) = \begin{Bmatrix} q_1(t) \\ q_2(t) \\ q_3(t) \end{Bmatrix} \quad (6)$$

Using simple steps, the previous eq.(3) can be written as:

$$\begin{aligned} \mathbf{\Phi}^T \mathbf{M} \mathbf{\Phi} \ddot{\underline{q}}(t) + \mathbf{\Phi}^T \mathbf{C} \mathbf{\Phi} \dot{\underline{q}}(t) + \mathbf{\Phi}^T \mathbf{K} \mathbf{\Phi} \underline{q}(t) &= \mathbf{\Phi}^T \mathbf{F}(t) \\ \rightarrow \mathbf{M}_q \ddot{\underline{q}}(t) + \mathbf{C}_q \dot{\underline{q}}(t) + \mathbf{K}_q \underline{q}(t) &= \mathbf{Q}(t) \end{aligned} \quad (7)$$

where $\mathbf{Q}(t) = \mathbf{\Phi}^T \mathbf{F}(t)$ is the generalize forces vector of the three considered modes and $\mathbf{M}_q, \mathbf{C}_q, \mathbf{K}_q$ are diagonal matrixes deriving respectively from the modal masses, damping ratio and natural frequencies of the structure.

The generalize force in its three cartesian components is calculated from the following equation:

$$Q_m^{x,y,z}(t) = \sum_k F_k^{x,y,z}(t) \cdot \phi_{m,k}^{x,y,z} \quad m = 1:3 \quad (8)$$

The total generalize force, for each modal mode, then is obtained as:

$$Q_m(t) = Q_m^x(t) + Q_m^y(t) + Q_m^z(t) \quad (9)$$

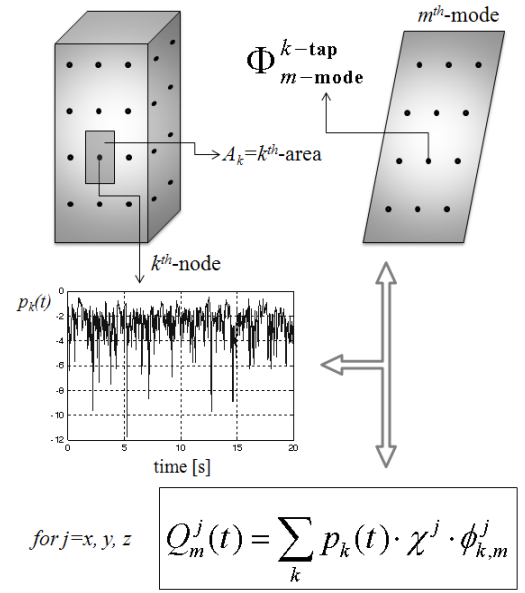
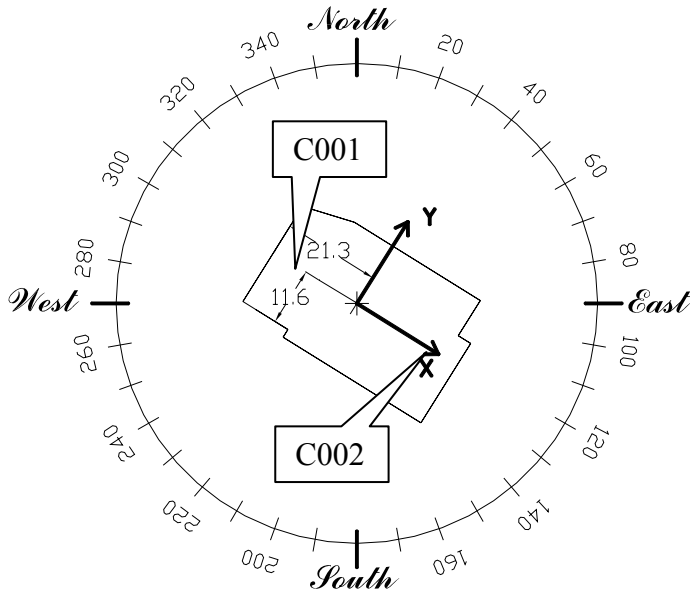


Figure 2. Tower position with respect to the north. Reference system for the forces, ground level. Positions of the comfort points C001 and C002, top floor (a). Diagram of the calculation of the generalized force of the m^{th} -mode (b).

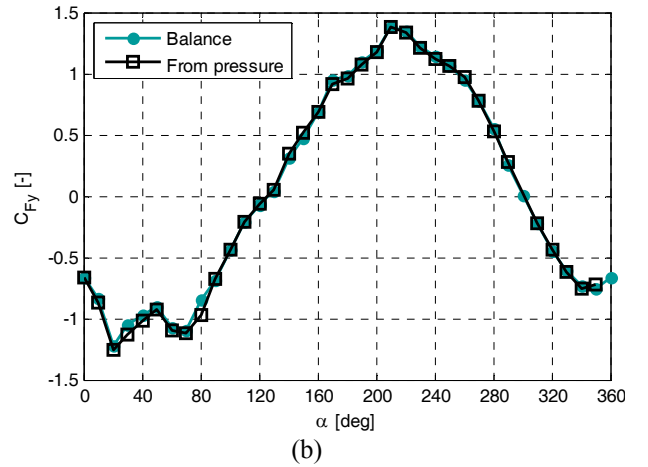
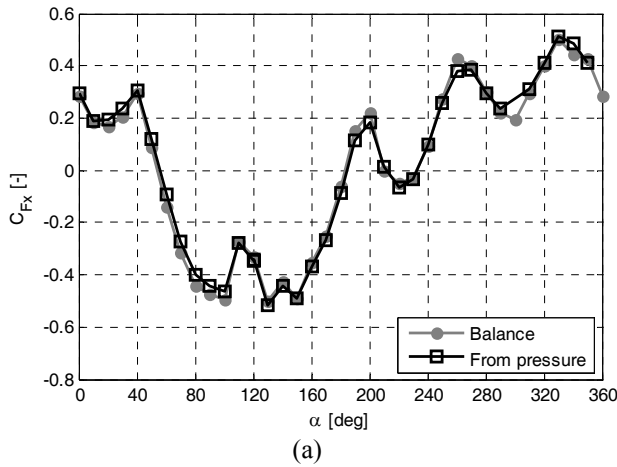


Figure 3. Force coefficient C_{FX} and C_{FY} in function of the wind exposition angle obtained from the balance and from the pressures: C_{FX} (a). C_{FY} (b).

By assuming the damping matrix \mathbf{C} to be a proportional damping, eq.(7), expressed in scalar form, results into three uncoupled equations (one for each mode considered in the analysis):

$$\left. \begin{aligned} m_{11}\ddot{q}_1(t) + c_{11}\dot{q}_1(t) + k_{11}q_1(t) &= Q_1(t) \\ m_{22}\ddot{q}_2(t) + c_{22}\dot{q}_2(t) + k_{22}q_2(t) &= Q_2(t) \\ m_{33}\ddot{q}_3(t) + c_{33}\dot{q}_3(t) + k_{33}q_3(t) &= Q_3(t) \end{aligned} \right\} \quad (10)$$

where m_{ii} , c_{ii} , and k_{ii} are generalized mass, generalized damping, and generalized stiffness of the m^{th} -mode respectively. The $q_m(t)$ are then solved from each of the above equations. Simulink is used

for the numerical solution of the above equations. Figure 2b show a diagram which summarizes the method used to calculated the generalized force. The response, in terms of displacements and accelerations of the real structure, can finally be evaluated using eq.(5).

The integral of the pressure over all the external area has to be coincident with the total force measured by the dynamometric balance. Figure 3 shows the comparison of the force coefficients C_{FX} , C_{FY} obtained from the balance and from the integration of the pressure: as one can see the agreement is excellent.

PEAK RESPONSE RESULTS

The peak values are calculated using the method of the peak factor for a Gaussian process. A detailed description of this method can be found for instance in Dyrbye (1996). The accelerations \ddot{X} are calculated in two point at the top-floor of the building representative for the comfort level in the tower (Figure 2a). Figure 4 shows an example of the response results, in term of peak acceleration in the point C002 in x and y directions. Three different values of damping ratio h were used in the simulations: $h=1\%$, 2% and 4% . In order to obtain a peak values important for the comfort level, a real wind speed with a return period of 5 year has been used in the simulations. The wind speed used in the simulation depends on the exposition angle: in this way it is possible to calculate the response of the building with very detailed.

Concerning the peak values in Figure 4, it is possible to see that the peak accelerations along the y -axis are greater. This is an effects of the combination of the first (lateral- x) and third (torsional) mode shapes. The effect of the torsional mode is considerable and so it is important to consider it in the analysis.

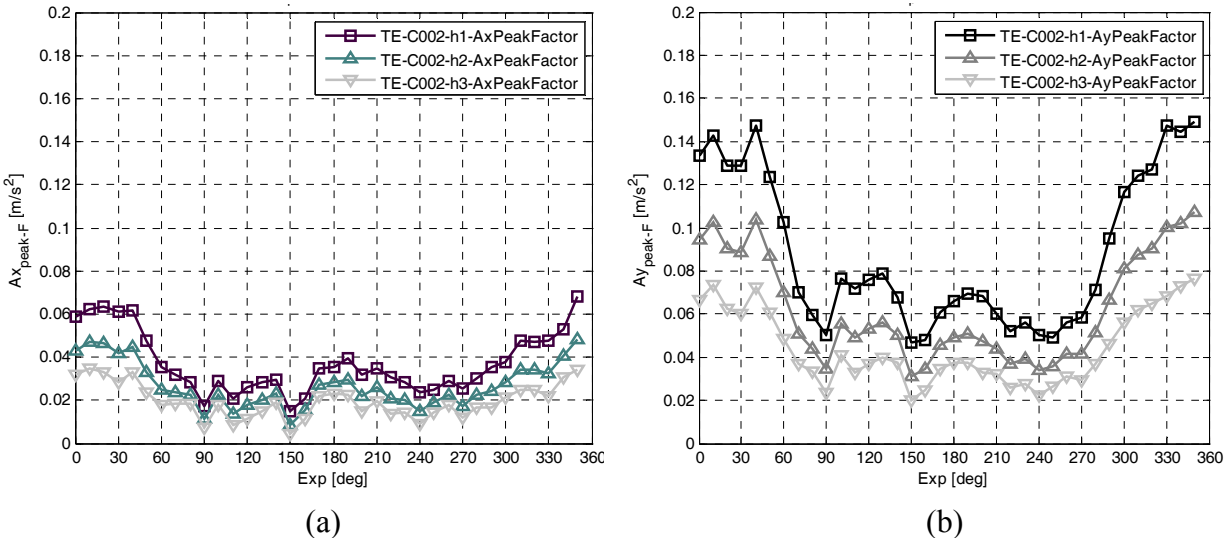


Figure 4. Point C002: peak-accelerations in x and y direction in function of the exposure angle. Damping $h=1\%$, 2% , 4% . x -direction (a). y -direction (b).

WIND LOADS

In order to evaluate the internal loads (shears, bending moments and torques) a lumped parameters model, whose masses correspond to the building storeys, has been adopted. The internal loads acting in correspondence of the nodes of the lumped parameters model are calculated considering the contribution of both the inertial loads and the external pressure forces due to the wind action on the building.

The outputs of this analysis are the internal loads at the base point for each wind exposure (Figure 2a) and the vertical distributions of both the internal loads and the corresponding virtual sectional loads (the virtual sectional loads are the loads to apply to the building in order to have the same shears, bending moments and torques), in correspondence of some interesting cases.

Inertial Loads

According to the modal approach described in the previous section, known the modal information (natural frequencies, modal masses and damping ratios) and calculated the lagrangian components of the external pressure forces, the response of the tower caused by the turbulent wind, is calculated in correspondence of the nodes of the lumped parameters model through the corresponding modal shapes. This allows, known the mass and the inertial data, the calculation of the inertial loads in each node. The analysis is carried out in the time domain, by step by step numerical integration of the motion equations of the tower, known the pressure measurements in correspondence of the pressure taps. As shown in the previous section, through the application of the modal approach, the motion equations result into three uncoupled equations, eq.(10).

Known the response in terms of generalized coordinates, it is possible to calculate accelerations (in x-direction, y-direction and z-rotation) of the nodes of the lumped parameters model through the following transformation of coordinates:

$$\ddot{\mathbf{X}}_{LP}(t) = \mathbf{\Phi}_{LP} \ddot{\mathbf{q}}(t) \quad (11)$$

where $\mathbf{X}_{LP}(t) = [\mathbf{x}_{LP}(t) \ \mathbf{y}_{LP}(t) \ \boldsymbol{\theta}_{zLP}(t)]^T$ is a $(3n_{LP} \times 1)$ vector: n_{LP} is the number of nodes of the lumped parameters model while \mathbf{x}_{LP} , \mathbf{y}_{LP} , $\boldsymbol{\theta}_{zLP}$ are vectors of time histories stories of displacements in x, y directions and rotation with respect to z direction. $\mathbf{\Phi}_{LP}$ is the $(3n_{LP} \times 3)$ matrix of eigenvectors relative to the nodes of the lumped parameters model and $\ddot{\mathbf{q}}(t)$ (3×1) is the vector of the time histories of the generalized accelerations.

The inertial loads (x-direction, y-direction and z-rotation) are then calculated, known the mass and the inertial properties, by the equations:

$$\mathbf{F}_{in}(t) = -\mathbf{M}_{LP} \cdot \ddot{\mathbf{X}}_{LP}(t) \quad (12)$$

where \mathbf{M}_{LP} is a square diagonal matrix $(3n_{LP} \times 3n_{LP})$:

$$\mathbf{M}_{LP} = \begin{bmatrix} m_1 & 0 & & & & & & & & 0 \\ 0 & m_2 & 0 & & & & & & & 0 \\ \vdots & \vdots & \vdots & \vdots & \vdots & \vdots & \vdots & \vdots & \vdots & \vdots \\ 0 & \dots & m_{n_{LP}} & 0 & & & \dots & & & 0 \\ 0 & \dots & & m_1 & 0 & & \dots & & & 0 \\ 0 & \dots & & 0 & m_2 & 0 & \dots & & & 0 \\ \vdots & \vdots & \vdots & \vdots & \vdots & \vdots & \vdots & \vdots & \vdots & \vdots \\ 0 & \dots & & & 0 & m_{n_{LP}} & 0 & \dots & & 0 \\ 0 & \dots & & & & 0 & J_1 & \dots & & 0 \\ 0 & \dots & & & & & 0 & J_2 & & 0 \\ \vdots & \vdots & \vdots & \vdots & \vdots & \vdots & \vdots & \vdots & \vdots & \vdots \\ 0 & \dots & & & & & & 0 & J_{n_{LP}} & \end{bmatrix} \quad (13)$$

while $\mathbf{F}_{in}(t)$ is the column vector of time-histories:

$$\mathbf{F}_{in}(t) = \begin{bmatrix} F_{in,x}^1(t) & F_{in,x}^2(t) & \dots & F_{in,x}^{N_{LP}}(t) \dots \\ \dots F_{in,y}^1(t) & F_{in,y}^2(t) & \dots & F_{in,y}^{N_{LP}}(t) \dots \\ \dots M_{in,z}^1(t) & M_{in,z}^2(t) & \dots & M_{in,z}^{N_{LP}}(t) \end{bmatrix}^T \quad (14)$$

External Pressure Loads

The time-history of the external forces is obtained by integrating the wind pressure over the corresponding effective surface area to give the six components of the force and moment. Starting from the same pressure time-histories measured in correspondence of the taps, the external pressure loads associated to the turbulent wind action are evaluated in correspondence of each node of the lumped parameters model by considering as reduction point the projection of the origin of the reference system (Figure 2a) at the height of the considered node.

For the k^{th} pressure tap, the external loads are then calculated by:

$$\begin{aligned} F_{ext,k}^i(t) &= p_k(t) \cdot \chi_k^i \\ M_{ext,k}^i(t) &= p_k(t) \cdot \chi_k^i \cdot h_k \quad i = x, y, z \end{aligned} \quad (15)$$

Internal loads

The internal loads (shears, bending moments and torque moments) are calculated as the integral of both the inertial and the external loads over the height of the building.

In particular, if we consider the j^{th} node (Figure 5), the inertial contribution to the internal load is calculated as the sum of the inertial loads $\mathbf{F}_{in}(t)$ acting on all the nodes having a z -coordinate higher than the vertical quote of the j^{th} node.

About the external loads contribution, as already described, each pressure tap is characterized by a tributary area: for the calculation of the internal loads at the j^{th} node, all the pressure taps, characterized by a tributary area having at least a point higher than the vertical quote of the j^{th} node, are considered. In particular, two cases can be considered: if all the points of the tributary area have a z -coordinate higher than the vertical quote of the j^{th} node, the external load contribution associated to the k^{th} pressure tap, calculated according to eq.(4), is all accounted for the calculation of the area. Besides, if only some points of the tributary area have a z -coordinate higher than the vertical quote of the j^{th} node, a new reduced tributary area $\tilde{\chi}$ is assigned to the pressure tap considering only the points having a z -coordinate higher than that of the j^{th} node.

The corresponding reduced external load is then calculated, for the s^{th} pressure tap, according to the following equations:

$$\begin{aligned} \tilde{F}_{ext,s}^i(t) &= p_s(t) \cdot \tilde{\chi}_s^i \\ \tilde{M}_{ext,s}^i(t) &= p_s(t) \cdot \tilde{\chi}_s^i \cdot h_s \quad i = x, y, z \end{aligned} \quad (16)$$

As shown in Figure 5a, the internal loads are calculated by making reference to the reduction point that coincides with the projection of the origin of the reference system (see Figure 2a).

The equations for the calculation of the internal loads at j^{th} node are the following (in the following, it has been considered that the numbers of the nodes of the lumped parameters model get from 1 to N_{LP} increasing the vertical quote z):

$$\begin{aligned}
F_{xTOT}(z_j, t) &= \sum_{n=j}^{N_{LP}} F_{in_x}^n(t) + \sum_k F_{ext_x}^k(t) + \sum_s \tilde{F}_{ext_x}^s(t) \\
F_{yTOT}(z_j, t) &= \sum_{n=j}^{N_{LP}} F_{in_y}^n(t) + \sum_k F_{ext_y}^k(t) + \sum_s \tilde{F}_{ext_y}^s(t) \\
M_{xTOT}(z_j, t) &= - \sum_{n=j}^{N_{LP}} F_{in_y}^n(t) * (z_n - z_j) + \sum_k M_{ext_x}^k(t) + \sum_s \tilde{M}_{ext_x}^s(t) \\
M_{yTOT}(z_j, t) &= \sum_{n=j}^{N_{LP}} F_{in_x}^n(t) * (z_n - z_j) + \sum_k M_{ext_y}^k(t) + \sum_s \tilde{M}_{ext_y}^s(t) \\
M_{zTOT}(z_j, t) &= \sum_{n=j}^{N_{LP}} M_{in_z}^n(t) - \sum_{n=j}^N F_{in_y}^n(t) * (x_n - x_j) + \sum_{n=j}^{N_{LP}} F_{in_x}^n(t) * (y_n - y_j) + \sum_k M_{ext_z}^k(t) + \sum_s \tilde{M}_{ext_z}^s(t)
\end{aligned} \tag{17}$$

where the index k refers to the pressure taps having the characteristics described at point 1 and while index s refers to that having the characteristics described at point 2.

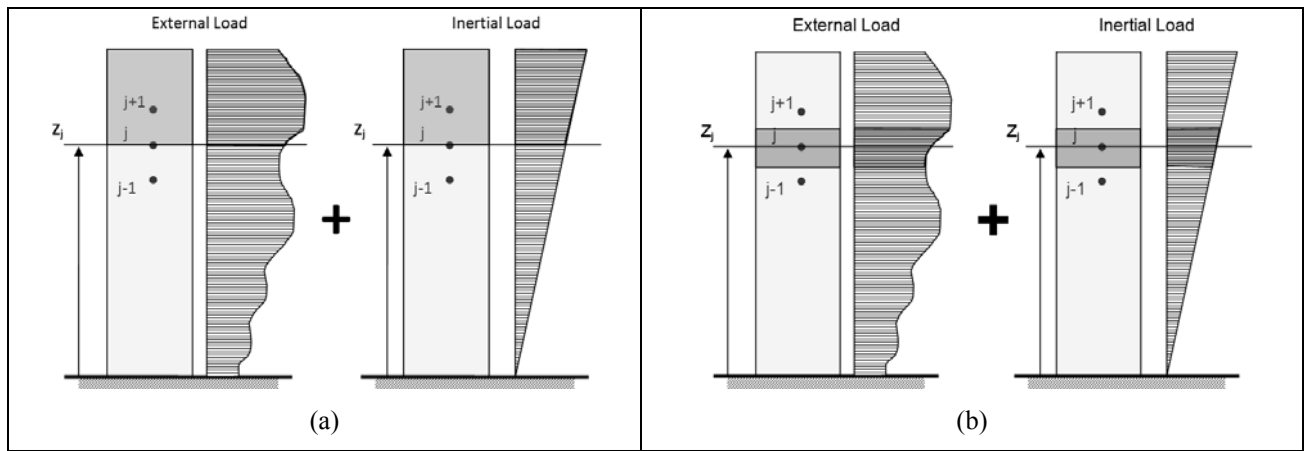


Figure 5. Calculation of the wind loads. Internal loads: external load plus inertial loads at the j^{th} node (a). Virtual sectional loads: external load plus inertial loads at the j^{th} node (b).

The virtual sectional loads to apply to the building to result in the same shears, moments and torques are then calculated, for the j^{th} node, as the sum of the inertial load calculated at the j^{th} node and the external load of the taps having at least a point whose vertical quote z is ranged between $z_{j, inf}$ and $z_{j, sup}$, where these two values are defined as (see Figure 5b):

$$\begin{aligned}
z_{j, inf} &= (z_j + z_{j-1}) / 2 \\
z_{j, sup} &= (z_j + z_{j+1}) / 2
\end{aligned} \tag{18}$$

Also in this calculation, the external loads are evaluated considering two cases: if all the points of the tributary area have a z -coordinate ranged between $z_{j, inf}$ and $z_{j, sup}$: the external load contribution associated to the k^{th} pressure tap is calculated according to eq.(4). Besides, if only some points of the tributary area have a z -coordinate ranged between $z_{j, inf}$ and $z_{j, sup}$, a new reduced tributary area $\hat{\chi}$ is assigned to the pressure tap considering only the points having a z -coordinate ranged between $z_{j, inf}$ and $z_{j, sup}$. The corresponding external load is then calculated, for the s^{th} pressure tap, according to the following equations:

$$\begin{aligned}
\hat{F}_{ext, s}^i(t) &= p_s(t) \cdot \hat{\chi}_s^i \\
\hat{M}_{ext, s}^i(t) &= p_s(t) \cdot \hat{\chi}_s^i \cdot h_s \quad i = x, y, z
\end{aligned} \tag{19}$$

The equations for the calculation of the virtual sectional loads at j-th node are the following:

$$\begin{aligned}
 F_{xsec}(z_j, t) &= F_{inx}^j(t) + \sum_k F_{extx}^k(t) + \sum_s \hat{F}_{extx}^s(t) \\
 F_{ysec}(z_j, t) &= F_{iny}^j(t) + \sum_k F_{exty}^k(t) + \sum_s \hat{F}_{exty}^s(t) \\
 M_{xsec}(z_j, t) &= \sum_k M_{extx}^k(t) + \sum_s \hat{M}_{extx}^s(t) \\
 M_{ysec}(z_j, t) &= \sum_k M_{exty}^k(t) + \sum_s \hat{M}_{exty}^s(t) \\
 M_{zsec}(z_j, t) &= M_{inz}^j(t) + \sum_k M_{extz}^k(t) + \sum_s \hat{M}_{extz}^s(t)
 \end{aligned}
 \tag{20}$$

Results

In order to evaluate the loads for structural design, the dynamic response of the tower is evaluated, through the modal approach over described, for a wind speed distribution characterized by a return period of 50 years. All 36 wind exposures simulated during the tests carried out in the wind tunnel are considered (Figure 2a): it is important to underline that the corresponding statistical base of equivalent full scale time is very wide (more than 30 hours full scale). In order to have the best frequency response of the numerical simulations, the lower wind test speed has been used.

As an example, Figure 8 shows the instant values of shears F_x vs. F_y (a) and of M_{xx} vs. M_{yy} (b) calculated at base point. From this figure, it is possible to highlight immediately the worst loads conditions to that the building is subjected for a wind characterized by a return period of 50 years. The selected points on the boundary of the region represent true instantaneous relative maximum values reached by the corresponding shear / bending moments at the building base. The external envelope of the points of each ‘cloud graphic’ is the reference base for selecting true wind loads distributions having the role of extreme values truly reached during a physically simulated event.

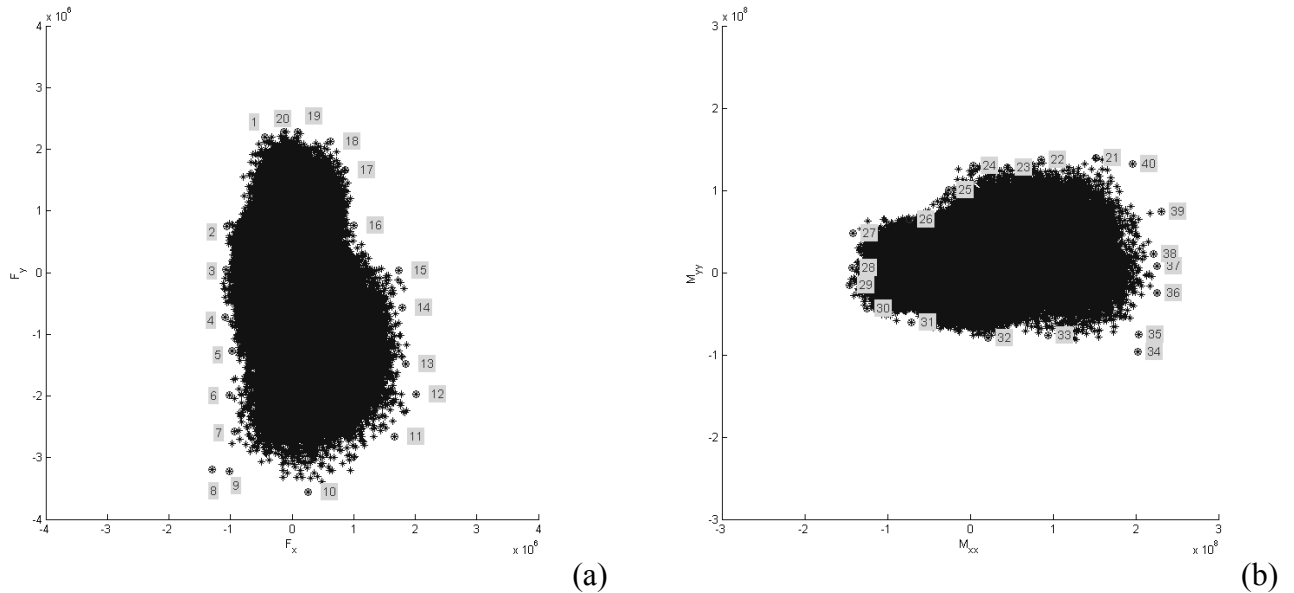


Figure 6: Instant values of the internal loads at base point. Shears F_y as a function of F_x (a) and bending moments M_{yy} as a function of M_{xx} (b) for all wind exposures: worst conditions identified (numbered points).

For each “load case”, the vertical distribution of the instant internal loads and virtual sectional loads can be calculated. Figure 7 shows, as instance, the vertical distribution of the shear F_y and of the virtual sectional load in y-direction in terms of comparison between the internal load and the corresponding components associated to the external pressure loads and to the inertial loads. To analyze shows the instantaneous external and inertial components separately: in this way the information concerning the instantaneous composition of the actual instantaneous overall load are available.

Finally, for two specific angles, $\alpha=330^\circ$ and $\alpha=120^\circ$, Figure 8 shows the vertical distribution of the mean value and of the maximum and minimum peak values of the shears F_y in terms of comparison between the total loads (triangular markers) and the components inertial loads (circular markers) and external pressure forces (solid line).

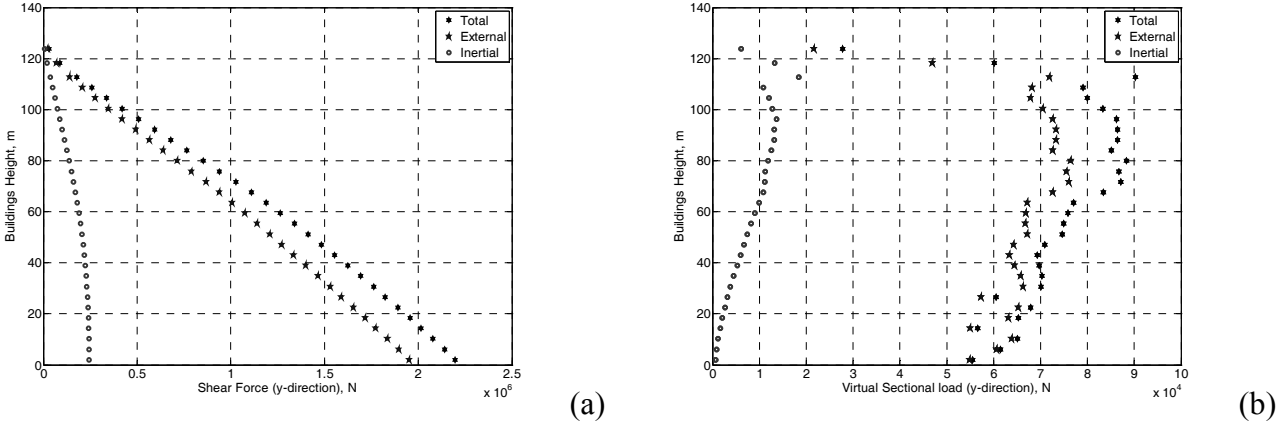


Figure 7: “Load case 1”: instantaneous vertical distribution of shear force F_y (a) and virtual sectional load in y-direction (b). Overall loads (six-star point), external pressure loads (star point) and inertial loads (circle points).

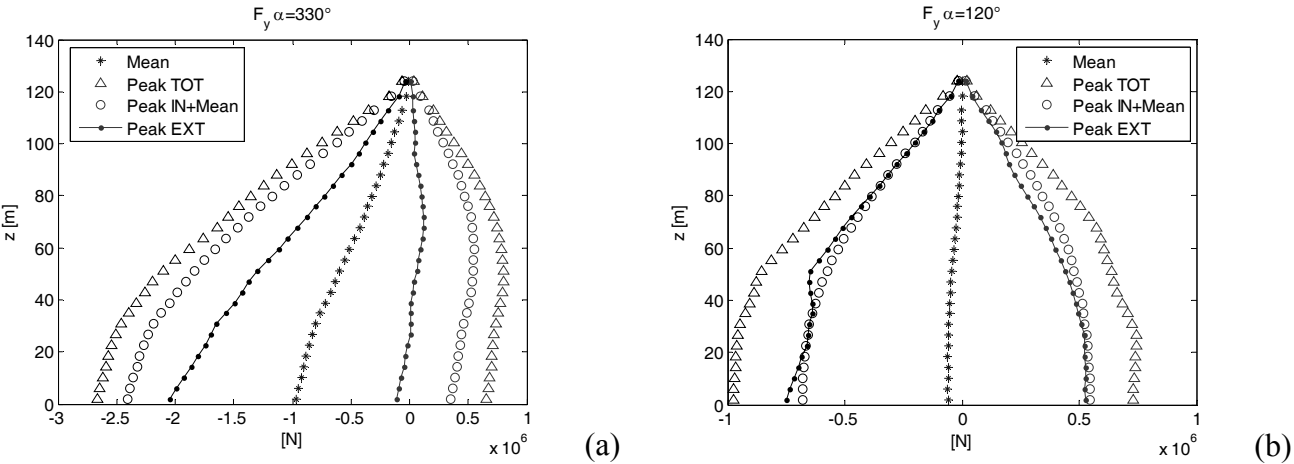


Figure 8: vertical distribution of mean (blu) and maximum (red) and minimum (black) peak values of the shear F_y for exposure angle $\alpha=330^\circ$ (a) and $\alpha=120^\circ$ (b). Total loads (triangular markers), inertial loads (circular markers) and external pressure forces (solid line).

At $\alpha=330^\circ$, the analysis of the accelerations in the frequency domain has shown that the three lower natural modes of the building are excited and the phenomenon of buffeting is present. At this angle the accelerations are very high due to the wind distribution that reaches around this angular sector its maximum value. From the force vertical distribution it is possible to observe that, also in this case, there is not a synchronization between the external forces associated to the pressure action on the building and the inertial forces and, as a consequence, the peak value of the total force at the different vertical quotes is not the sum of the peak values associated to the external forces and to the inertial loads. At $\alpha=120^\circ$, the phenomenon of vortex shedding arises along the y-axis; contemporary, a resonant pick associated to the first natural frequency of the building is present. As a consequence, there is a superposition of both buffeting effects (at the natural frequency) and vortex shedding that do not allow a significant synchronization between the external forces associated to the pressure action on the building and the inertial forces.

CONCLUSIONS

Developments in civil and mechanical engineering have led to designs that satisfy strength requirements but that are often very flexible. These flexibilities could lead unfavorable dynamic responses on the occupants comfort when the structure is subjected to dynamic loads like turbulent winds

The method described in this article shows how it is possible to combine a modal approach analysis, with experimental wind tunnel test in order to simulate the dynamic of a tall building, and suggests a procedure for the identification of significant "load cases" to be used as references for structural evaluations. These "load cases", accounting for the external loads as well as the inertial loads, evidence the very different role played by the inertial loads in determining the load conditions, depending on the wind interaction characteristics, i.e. the exposure angle or vortex shedding effects.

REFERENCES

- ASCE, American society of civil engineers (2008). "Minimum design loads for buildings and other structures. SEI/ASCE 7-02", Reston, Virginia.
- Eurocode 1, (2004). "Actions on structures - Part 1-4: General actions - Wind actions. prEN 1991-1-4, European Standard.
- NatHaz, (2008). Aerodynamic Loads Database, <http://aerodata.ce.nd.edu/>.
- C. S. Kwok, (2008). "Motion simulator study on effects of wind-excited tall building motion on occupants" presented at Wind effects on buildings and urban environment, Tokio, Japan.
- Claës Dyrbye & Svend Ole Hansen, (1996). "Wind Loads on Structures". John Wiley & Sons (Hardcover).